

Experiments and calculations on the illumination of spherical microtargets by a terawatt iodine laser

E. N. Avrorin, V. A. Eroshenko, A. I. Zaretskiĭ, A. I. Zuev, S. B. Kormer, G. G. Kochemasov, V. B. Kryuchenkov, V. A. Lykov, V. M. Murugov, A. V. Ryadov, A. V. Senik, and S. A. Sukharev

(Submitted 2 January 1984)

Zh. Eksp. Teor. Fiz. **87**, 417–421 (August 1984)

The gas-dynamic program “Zarya” was used to analyze and interpret experimental data on the irradiation of spherical microtargets, filled with DT gas, by an iodine laser in the Iskra-IV system. Reasonable agreement was demonstrated between calculations and experiment. A yield of 10^8 neutrons per pulse is predicted by calculations based on the optimization of focusing and an increase in the laser power at the target up to the maximum of 2 TW that can be attained in the Iskra-IV system.

Experiments have continued with the Iskra-IV system¹ on the compression of spherical microtargets filled with DT gas by radiation from an iodine laser operating at $\lambda = 1.315 \mu\text{m}$. The first experiments performed under the “exploding shell” conditions have already been reported.² In this paper, calculations performed by the “Zarya” program³ are used to interpret both previously published experiments and those performed in 1981. Calculations on the optimization of targets in the Iskra-IV system are also presented.

The laser power per pulse sent to the target was varied in the range 0.8–1.7 TW with pulse lengths $\tau_{1/2}$ in the range 250–450 ps and energy E_L in the range 264–630 J. The light beam produced at exit from the single-channel Iskra-IV system, which has an aperture of 270 mm, was divided by light-splitting plates into four beams which were then directed onto the microtarget by parabolic mirrors with focal length $f = 270 \text{ mm}$, placed at the corners of a tetrahedron. The diameter of the ray caustic at the 80% energy level was 150–180 μm . The beams could be focused on the target to within about 20 μm in the transverse direction and about 30–50 μm in the longitudinal direction. The energy and power contrast of the laser radiation was $K_E \gtrsim 10^7$ and $K_p \gtrsim 10^6$, respectively.

Calculations were compared with experiments, using data on the energy absorbed by the target, x-ray spectra, and neutron yields. The experimental absorption coefficient was determined from calorimetric measurements of laser energy on the target (incident, reflected, and scattered) and the energy of x rays and corpuscular particles in the expanding plasma. The sensitivity threshold of neutron methods was about 10^4 neutrons per pulse. The compression symmetry was examined with an x-ray pinhole camera having a resolution of 20–30 μm . The continuous x-ray spectrum in the photon energy range 1–60 keV was determined by using gray and K filters. Line spectra due to multiply-charged silicon ions were examined with a mica-crystal spectrograph. The targets used in these experiments were glass shells with diameter $2R_0 = 150\text{--}170 \mu\text{m}$ and wall thickness $\Delta = 0.7 + 1.5 \mu\text{m}$. The variation in the wall thickness was 3–5% and the targets were filled with DT gas to a pressure $P_0 = 10\text{--}14 \text{ atm}$. The energy flux density of the laser radiation at the target was about $10^{15}\text{--}2 \times 10^{15} \text{ W/cm}^2$. The fraction K_a of ab-

sorbed laser energy varied from 10 to 16% in most experiments. In the series of 11 experiments considered here, the neutron yield lay in the range $N = 10^4\text{--}10^5$ in six of them and $N = 10^5\text{--}10^6$ in the other five. A yield of 10^6 (2×10^6 neutrons per pulse) was recorded in one experiment. Figure 1

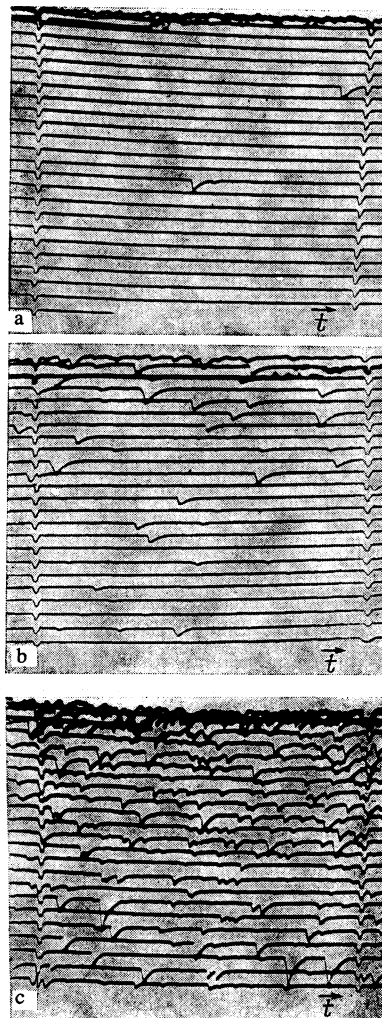


FIG. 1. Oscillograms of the measured neutron yield, obtained by the delayed recording method: a— $N \approx 10^4$, b— $N = 1.5 \times 10^5$, c— $N = 2 \times 10^6$.

shows typical oscillograms recorded in experiments with $N = 10^4$, 1.5×10^5 , and 2×10^6 . In all these experiments, the recorded x-ray spectra had a well-defined two-temperature shape with $T_c \simeq 0.6-1$ keV and $T_n = 9-14$ keV. The total soft x-ray energy was $E_{sx} \simeq 2-5$ J (or about 5-10% of the energy absorbed by the target), whereas the energy of hard x rays with $\epsilon_\gamma \gtrsim 10$ keV was $E_{hx} \simeq 0.4-10$ mJ. Analysis of the line spectra due to multiply charged silicon ions showed that the average electron temperature in the corona was close to the values T_c found from continuous spectra. The x-ray radiation was also recorded with a pinhole camera in a series of experiments reported elsewhere.² These data indicated that volume compression by a factor of 30-60 was achieved but, in most experiments with the pinhole camera, the image was in the form of a luminous ring or disk without a well-defined central emission. We note that no correlation was established between the neutron yield and the appearance of the central emission on the images recorded with the camera obscura.

The table lists experimental parameters and results of the 11 experiments mentioned above. It also gives the results of one-dimensional calculations performed in the "Zarya" program.³

The "Zarya" program is based on a model of the interaction between the laser radiation and the corona. It is used to calculate absorption, taking into account focusing conditions, compression of the density profile, refraction of laser radiation, resonance, parametric, backward inverse bremsstrahlung and SMBS. The single-group transport equation was used to describe the transport of energy by fast electrons produced as a result of resonance and parametric absorption. The diffusional electronic heat flux was limited in these calculations to a maximum of $q_e^* = f n_e T_e (T_e/m_e)^{1/2}$ with $f = 0.1$.

The program was checked against the series of experiments performed on a neodymium-glass Janus, Argus, and Chroma systems⁴ with gas-filled targets and different current densities, wavelengths, pulse lengths, and laser-beam focusing conditions. It was found that there was good agreement between calculations and experimental data on the absorbed energy, neutron yield, x-ray spectra, and volume compression.

The table lists experimental data obtained with Iskra-IV, together with computed results obtained for the given laser-pulse parameters and focusing conditions. The physicomathematical model was corrected for the wavelength difference ($\lambda = 1.315 \mu\text{m}$ instead of $\lambda = 1.06 \mu\text{m}$), but the remaining parameters were allowed to remain the same.

The line intensities due to the hydrogen- and helium-like silicon ions and their satellites were calculated from the nonstationary coronal model of the ion composition of SiO_2 plasma. The calculated x-ray line intensities were used by analogy with Ref. 5 to determine the temperature T_{1c} from the ratio of the satellites j, k, l to the intensity of the line w , and T_{2c} from the ratio of the total intensity of the satellites G, Q, M, X, Y, V to the L_α line intensity. The experimental and calculated temperatures are listed in Table I.

It is clear from the table that there is reasonable agreement between calculations and experiments for practically all the parameters, with the exception of the neutron yield in a number of the experiments. According to the calculations, the fraction of absorbed laser energy was 16-21% (the measured values were 10-19%, depending on the focusing condition). The corresponding calculated resonance absorption coefficient is 13-17% and the parametric and inverse-bremsstrahlung absorption is small. Reflection due to SMBS scattering is also small and does not exceed 10%. Heating of the target by fast electrons with an effective temperature of

TABLE I. Results of experiments performed on Iskra-IV and calculations performed by program "Zarya."

No. of expt.	$2R_0, \mu\text{m}$	$\Delta, \mu\text{m}$	P_0, atm	E_L, J	$\tau_{1/2}, \text{ns}$	$\frac{K_a^e}{K_a^c}$	$\frac{N_e, 10^4}{N_c, 10^4}$	δ	$\frac{T_n^e}{T_n^c}$	$\frac{T_{1c}^e}{T_{1c}^c}$	$\frac{T_{2c}^e}{T_{2c}^c}$	$\frac{E_{sx}^e}{E_{sx}^c}$	$\frac{E_{hx}^e}{E_{hx}^c}$	$W = \frac{N^c}{N_e}$
09 041	153	1.1	34	275	0.32	$\frac{16}{18}$	$\frac{0.16}{0.64}$	41	$\frac{9}{8}$	$\frac{0.36}{0.57}$	$\frac{0.78}{0.78}$	$\frac{2}{3.1}$	$\frac{1.6}{0.8}$	1.7
22 041	162	0.7	32	380	0.34	$\frac{13}{19}$	$\frac{0.01}{18}$	34	$\frac{9}{9}$	$\frac{0.36}{0.63}$	$\frac{0.63}{0.85}$	$\frac{2.7}{4.1}$	$\frac{1.3}{1.4}$	300
08 051	166	1.2	35	410	0.45	$\frac{15}{21}$	$\frac{0.015}{0.85}$	40	$\frac{10}{9}$	$\frac{0.39}{0.60}$	$\frac{0.65}{0.90}$	$\frac{3.6}{4.5}$	$\frac{2}{1.6}$	15
15 051	162	1.1	11	375	0.45	$\frac{12}{21}$	$\frac{0.02}{5}$	275	$\frac{8}{9}$	$\frac{0.38}{0.62}$	$\frac{0.54}{0.89}$	$\frac{2.7}{8}$	$\frac{1}{1.7}$	15
21 051	160	0.8	30	350	0.54	$\frac{12}{18}$	$\frac{0.01}{2.3}$	50	$\frac{9}{8}$	$\frac{0.45}{0.63}$	$\frac{0.55}{0.90}$	$\frac{2.7}{3.8}$	$\frac{1.3}{1.4}$	15
24 061	150	0.9	31	525	0.38	$\frac{17}{19}$	$\frac{2}{5.4}$	47	$\frac{13}{15}$	$\frac{0.5}{0.57}$	$\frac{0.75}{0.79}$	$\frac{2.2}{4.7}$	$\frac{10}{2.2}$	1.5
23 071	170	1.2	21	630	0.37	$\frac{13}{16}$	$\frac{0.15}{2.2}$	61	$\frac{14}{17}$	$\frac{0.38}{0.51}$	$\frac{0.7}{0.78}$	$\frac{3.8}{6.5}$	$\frac{8}{3}$	5
31 071	159	0.7	25	264	0.31	$\frac{14}{21}$	$\frac{0.015}{3.2}$	36	$\frac{13}{11}$	$\frac{0.38}{0.53}$	$\frac{0.59}{0.73}$	$\frac{2.7}{3.2}$	$\frac{5}{0.8}$	20
17 091	158	1.5	17	284	0.28	$\frac{19}{20}$	$\frac{0.01}{0.7}$	50	$\frac{10}{13}$	$\frac{0.38}{0.50}$	$\frac{0.65}{0.71}$	$\frac{4}{4}$	$\frac{0.4}{1.5}$	70
29 101	165	1	35	380	0.23	$\frac{10}{19}$	$\frac{0.14}{7}$	28	$\frac{11}{14}$	$\frac{0.41}{0.42}$	$\frac{0.7}{0.64}$	$\frac{4.5}{5.3}$	$\frac{1.7}{1.6}$	3
20 111	162	0.8	22	433	0.25	$\frac{10}{19}$	$\frac{0.5}{1.80}$	61	$\frac{13}{15}$	$\frac{0.34}{0.44}$	$\frac{0.7}{0.7}$	$\frac{5}{5}$	$\frac{3.5}{2.6}$	8

* Experimental and calculated values are indicated by the symbols e and c, respectively.

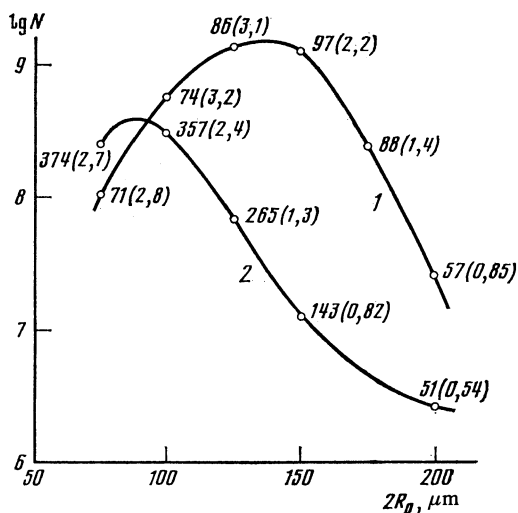


FIG. 2. Neutron yield as a function of the diameter of the glass shell for $P_L = 2$ TW, $\tau_{1/2} = 0.25$ ns, and focal spot diameter of 150 μm : curve 1—shell aspect ratio $R/\Delta = 100$, 2— $R/\Delta = 50$; the temperature of the DT mixture under compression T_i (keV) (numbers in parentheses) is shown together with the maximum volume compression δ . The initial density of the DT mixture is $\rho_0 = 0.0035$ g/cm³.

about 10–15 keV leads to a compression of the target under the “exploding shell” regime, with a volume compression of about 40–60. Good agreement is obtained with x-ray spectra. Some discrepancy in T_{1c} can be explained by the fact that self-absorption in the line w was not taken into account. As far as discrepancy between the measured (N^e) and calculated (N^c) values of the neutron yield are concerned, calculations of the latter show that, since $N^c \propto K_a^7$, where K_a is the fraction of absorbed energy, a reduction in the fraction of absorbed energy down to the measured values ensures that the ratio W of the calculated N^c to the measured N^e yield for five out of the 11 experiments becomes 1.5–8, whereas the result is 15–20 for four of the experiments and 70 and 300, respectively, for the remaining two.

The discrepancy between the values of N can be explained to within an order of magnitude by the fact that the calculations were based on a one-dimensional model, i.e., no account was taken of the nonuniform illumination of the targets and the variation in the thickness of the shells, which leads to an asymmetry in the compression, thus reducing neutron yields. The reason for the discrepancy between N^e and N^c by two orders of magnitude in two of the experiments is not as yet clear.

One comparison of the calculations and experiments has given us greater confidence in the recommendations that can be based on these calculations.

Figure 2 shows the calculated compression of gas-filled shells for the following parameters that can be attained in the Iskra-IV system: $P_L \simeq 2$ TW, $\tau_{1/2} = 0.25$ ns, and focal spot diameter 150 μm . The initial density of DT gas was held constant in these calculations, and the shell parameters were varied in order to determine the optimum target with respect to the neutron flux. As can be seen from Fig. 2, when the shell diameter is 120–160 μm and the aspect ratio if $R/\Delta \simeq 100$, the calculated neutron flux for Iskra-IV is up to about 10^9 neutrons per pulse under optimum focusing conditions and laser power at the target up to 2 TW. A neutron flux of 10^7 – 10^8 neutrons per pulse may be expected in practice, so that more complete physical investigations will become possible.

¹S. B. Korner, *Izv. Akad. Nauk SSSR Ser. Fiz.* **44**, 2002 (1980).

²F. M. Abzaev, N. N. Beznasyuk, V. G. Bezuglov *et al.*, *Zh. Eksp. Teor. Fiz.* **82**, 459 (1982) [*Sov. Phys. JETP* **55**, 263 (1982)].

³E. N. Avrorin, V. I. Zuev, N. G. Karlykhanov, V. A. Lykov, and V. E. Chernyakov, *Pis'ma Zh. Eksp. Teor. Fiz.* **32**, 457 (1980) [*JETP Lett.* **32**, 437 (1980)].

⁴E. Storm *et al.*, *Phys. Rev. Lett.* **40**, 1570 (1978); E. Storm *et al.*, *J. Appl. Phys.* **49**, 959 (1978); D. Slater *et al.*, *Phys. Rev. Lett.* **46**, 18, 1199 (1981).

⁵A. S. Ganeev, A. L. Zapysov *et al.*, *Kvantovaya Elektron. (Moscow)* **7**, 2227 (1980) [*Sov. J. Quantum Electron.* **10**, 1294 (1980)].

Translated by S. Chomet